

Implementation of probabilistic algorithms by multi-chromophoric molecular networks with application to multiple travelling pathways

Barbara Fresch¹, F. Remacle^{2,3}, R. D. Levine^{3,4}

¹ *Department of Chemical Science, Via Marzolo 1, 35131, University of Padova, Italy*

² *Department of Chemistry, B6c, University of Liege, B4000 Liege, Belgium*

³ *The Fritz Haber Center for Molecular Dynamics and Institute of Chemistry, The Hebrew University of Jerusalem, Jerusalem 91904, Israel*

⁴ *Crump Institute for Molecular Imaging and Department of Molecular and Medical Pharmacology, David Geffen School of Medicine and Department of Chemistry and Biochemistry, University of California, Los Angeles, California 90095, United States.*

Abstract

The implementation of probabilistic algorithms by deterministic hardware is demanding and requires hundreds of instructions to generate pseudo-random sequence of numbers. On the contrary, the dynamics at the molecular scale is physically governed by probabilistic laws because of the stochastic nature of thermally activated and quantum processes. By simulating the exciton transfer dynamics in a multi-chromophoric system we demonstrate the implementation of a random walk that samples the possible pathways of a traveler through a network and can be probed by time resolved fluorescence spectroscopy. The ability of controlling the spatial arrangement of the chromophores allows us to design the “landscape” in which the traveler is moving and therefore to program the molecular device.

Keywords: Molecular logic, random walk, FRET, time resolved spectroscopy

1. Introduction

Random walks and Markov chains are one of the cornerstones of computer science.^[1] As algorithmic tools they are applied to solve central problems like searching and ranking contents through the web^[2], analyzing social behaviors^[3] or modelling the evolution of DNA and protein sequences.^[4] They provide a general paradigm for sampling and exploring combinatorial structures by using a sequence of simple, local transitions.^[5] The implementation of probabilistic algorithms by deterministic hardware is highly inefficient, requiring significant overhead at each step. For example, the mere sampling a pseudo-random number from a probability distribution requires hundreds of instructions. A natural alternative is to propose computing hardware whose physical dynamics are ruled by probabilistic law.^[6] Physical systems satisfying this requirement are indeed quite common at the nano-scale where randomness is associated with both the variability of nano-devices in terms of structure and properties^[7] and to the fundamental stochastic nature of thermally activated and quantum processes. As we will discuss in detail throughout this work, the dynamics of molecular systems is often a rather straightforward implementation of a random walk algorithm. The challenge resides in how to control and set up an application-specific algorithm and how to extract the relevant information as output from a molecular system. In this contribution, we discuss a possible route to exploit the randomness of a realistic chemical system: the exciton transfer dynamics in multi-chromophore molecular aggregates. Multi-chromophore compounds have been already recognized as promising candidates for photonics applications in molecular based logic^[8], data storage^[9], sensing^[10] and light harvesting devices.^[11] Central to their technological relevance is the ability of positioning fluorophores with a spatial precision down to 4 Å. Many of the multi-chromophoric systems that have been designed and experimentally realized, see for example refs.^[11a-c, 12], took advantage of the impressive developments of the DNA nanotechnology.^[13] DNA scaffolds provide a flexible means for organizing fluorophores into specific patterns to create useful functionality. Further, the ability to program DNA into complex three-dimensional shapes^[14] allows the fluorophore network to be configured into virtually any three-dimensional arrangement. Moreover, specialized fluorescent molecules for DNA labelling are commercially available, they can be covalently conjugated to one or more nucleotides via aliphatic linkers or bound to the DNA scaffold through non-covalent interaction including intercalation^[15]. Time-resolved fluorescence analyses by time correlated single-photon counting (TCSPC) and streak camera techniques are able to reveal the cascading energy transfer

processes between different dyes typically on the picosecond time scale and even at the single molecule level.^[16]

In this work, we will show that the hopping dynamics of excitons in a multi-chromophore system implements a random walk that samples the possible pathways of a traveler through a network of cities. The ability of controlling the spatial arrangement of the chromophores allows us to program the “landscape” in which the traveler is moving and the connections between cities. Time (and frequency) resolved fluorescence spectra are the output of the multi-chromophore device. We will show how time resolved fluorescence signal encodes the relevant information about the possible pathways followed by the traveler: the probability of reaching a specific city, the time that it will likely take and the effect of starting the journey from different locations. We present a proof of principle by considering a rather simple chromophoric system composed of a triad of dyes. However, the same concepts can be easily applied to systems of complex and customizable topology. For example, natural light-harvesting systems consist of hundreds of thousands scaffolded chromophores.

The paper is organized as follows: in the next section we outline the physical description of the energy transfer dynamics in multi-chromophore systems based on Förster theory^[17] and how such dynamics determines the time resolved fluorescence signal. In section 3 we discuss in details the correspondence between the physical process of exciton transfer and the implementation of a Markov chain that realizes a random walk. In section 4 we demonstrate that the physical implementation of the algorithm can be applied to solve a real life-like problem through the analysis of the possible paths through the state space of the problem. In the concluding section, we outline the possible developments of our approach to logic processing at the molecular scale.

2. Förster energy transfer in chromophoric networks

Upon photoexcitation, a dye molecule is in its electronic excited state and therefore an exciton is created. Multiple de-excitation mechanisms are in principle possible depending on the nature of the chromophore and its environment. The processes that are of interest to us are emission by fluorescence, non-radiative decay and energy transfer to other dye molecules. In the absence of any inter-chromophore transfer, the intensity of the fluorescence emission is proportional to the quantum yield of the dye $\Phi_i = \Gamma_i / (\mathbf{K}_{nr,i} + \Gamma_i)$, where Γ_i is the emission rate and $\mathbf{K}_{nr,i}$ the rate of non-

radiative decay. The fluorescence signal decays in time exponentially according to the lifetime of the excited state $\tau_i = (\mathbf{K}_{nr,i} + \Gamma_i)^{-1}$. If the electronic coupling between different dyes in the system is weak compared to the homogeneous spectral line broadening, which is appropriate for inter-dye separations on the order of or greater than ~ 2 nm,^[18] energy migration may accurately be described using FRET (Förster resonant energy transfer) theory.^[17, 19] In a multi-chromophore system of n dyes, each dye is energetically coupled to the other $n-1$ dyes. The temporal evolution of the exciton population p_i , with $i=1, \dots, n$, is described by a kinetic equation,

$$dp_i/dt = \sum_{i,j \neq i}^n \mathbf{K}_{ij} p_j - \sum_{i,j \neq i}^n \mathbf{K}_{ji} p_i - \mathbf{K}_{ii} p_i \quad (1)$$

The first two terms on the r.h.s of eq.(1) account for the energy transferred to dye i from other dyes $j \neq i$ and the energy transferred from dye i to other dyes. The third term $\mathbf{K}_{ii} = \Gamma_i + \mathbf{K}_{nr,i}$ describes the energy loss because of exciton recombination either by emission (with rate Γ_i) or non-radiative decay (with rate $\mathbf{K}_{nr,i}$). The off diagonal components of the kinetic matrix \mathbf{K} of eq.(1) are the energy transfer rates between dyes and they are given explicitly as

$$\mathbf{K}_{ij} = \frac{1}{\tau_j} \left(\frac{R_{0,ij}}{|r_{ij}|} \right)^6 \quad (2)$$

where τ_j is the lifetime of the chromophore that acts as donor, $R_{0,ij}$ is the critical Förster distance, that is the distance at which the transfer efficiency is 50%, and r_{ij} is the distance between the two chromophores. The parameter $R_{0,ij}$ depends on the photo-physical properties of the dyes and their respective orientation, namely $R_{0,ij} = [8.8 \cdot 10^{23} \cdot \kappa^2 \cdot n^{-4} \cdot \Phi_j \cdot J_{ij}]^{1/6}$ where J_{ij} denotes the monomeric spectral overlap, κ the dipole orientation factor (that we will set equal to $2/3$ assuming the validity of an isotropic average on the relative orientations) and n is the refractive index of the surrounding medium.

Let us introduce our simple logic units composed by three chromophores. In this case, we have three excited state populations and the kinetic matrix \mathbf{K} is a 3 by 3 matrix. Similarly to the model of light harvesting antenna assembled by Dutta et al in a DNA scaffold,^[11b] we choose three dyes

characterized by well separated excitation/emission spectra (reported in Figure 1A), namely Pacific Blue (Blue) Alexa Fluor 555 (Yellow) and Alexa Fluor 647 (Red). With this choice, we can selectively excite only one of the three dyes by tuning the excitation wavelength and we can selectively read out the fluorescence emitted by a specific dye by reading the signal at the corresponding emission frequency. This will be important for the logic application discussed below since it allows controlling the inputs (excitation) and provides a direct reading of the output (fluorescence) of our molecular device. The dynamics of the exciton transfer clearly depends on the spatial arrangements of the dyes as the transfer rates eq. (2) strongly depends on the inter-dye distances. We start by considering a triangular geometry as depicted in figure 1B. The elements of the kinetic matrix are calculated from the photo-physical properties of the dyes (see table 1).

Table 1: Photo-physical properties of the dyes used in our model. Data of the Pacific Blue dye (Blue) are taken from^[11d] while data of the Alexa Fluor dyes (Yellow and Red) were retrieved from Invitrogen website.^[20]

	Φ	$\tau(\text{ns})$	$\lambda_{\text{max}} \text{ Abs (nm)}$	$\lambda_{\text{max}} \text{ Em (nm)}$
Blue (PB)	0.75	2.6	416	451
Yellow (AF555)	0.1	0.3	555	565
Red (AF647)	0.33	1.0	647	668

The macroscopic output of the multi-chromophore network is given by the time resolved fluorescence signal.^[21] Time Correlated Single Photon Counting (TCSPC) measurements are based on the detection of the arrival times of individual photons after optical excitation of a sample. It makes use of a pulsed excitation source (typically laser or LED). Production of a light pulse triggers the timing electronics that are stopped by a signal from the detector when a fluorescence photon is recoded. The photons are binned according to their arrival time giving the histogram of the time resolved photon counts. By using a streak camera to detect photons the signal is dispersed by wavelength so that the entire two-dimensional (spectro-temporal) data is collected in a single experiment. Additionally, streak camera is faster than TCSPC allowing time resolution down to 1 ps. The expected photon counts at the emission wavelength λ at time t is proportional to the excited state populations

$$I(\lambda, t) = \sum_i \Gamma_i p_i(t) Em_i(\lambda) \quad (3)$$

where $Em_i(\lambda)$ is the normalized emission spectra at the detection wavelength and the time evolution of the populations is given by the rate equation (1). The steady state emission spectrum is recovered by taking the long time integral of eq. (3). Figures 1C and D shows the calculated time resolved fluorescence spectrum of the chromophore triad for two different geometrical arrangements by setting the excitation wavelength to the absorption of Pacific blue. The inset on each panel shows the corresponding steady state fluorescence spectrum. In the first geometry, the distance r between the yellow dye (AF647) and the red dye (AF555) is set equal to 3nm (while the other two distances are 2.5 nm and 3nm, see figure 1B). The fluorescence of Pacific blue decays during the first 200ps after excitation and the fluorescence of the red dye increase reaching their maximum in the same timescale. The signal of the yellow dye is very weak reflecting a small exciton population of its excited state. In the nanosecond timescale the fluorescence signal extinguishes in agreement with the lifetime of the excited state of the red dye. By moving the yellow dye further apart from the red dye ($r=5\text{nm}$) without changing the other distances we obtain a nearly linear arrangement. The time resolved fluorescence signal changes as shown in panel D: the signal of pacific blue is practically unaffected while the fluorescence of red dye increases on a slower time-scale. Now the yellow fluorescence is enhanced reflecting an increasing population of the AF555 excited state. Clearly the excitons that reach the yellow dye are now less easily transferred to the red dye because of the increased distance between them.

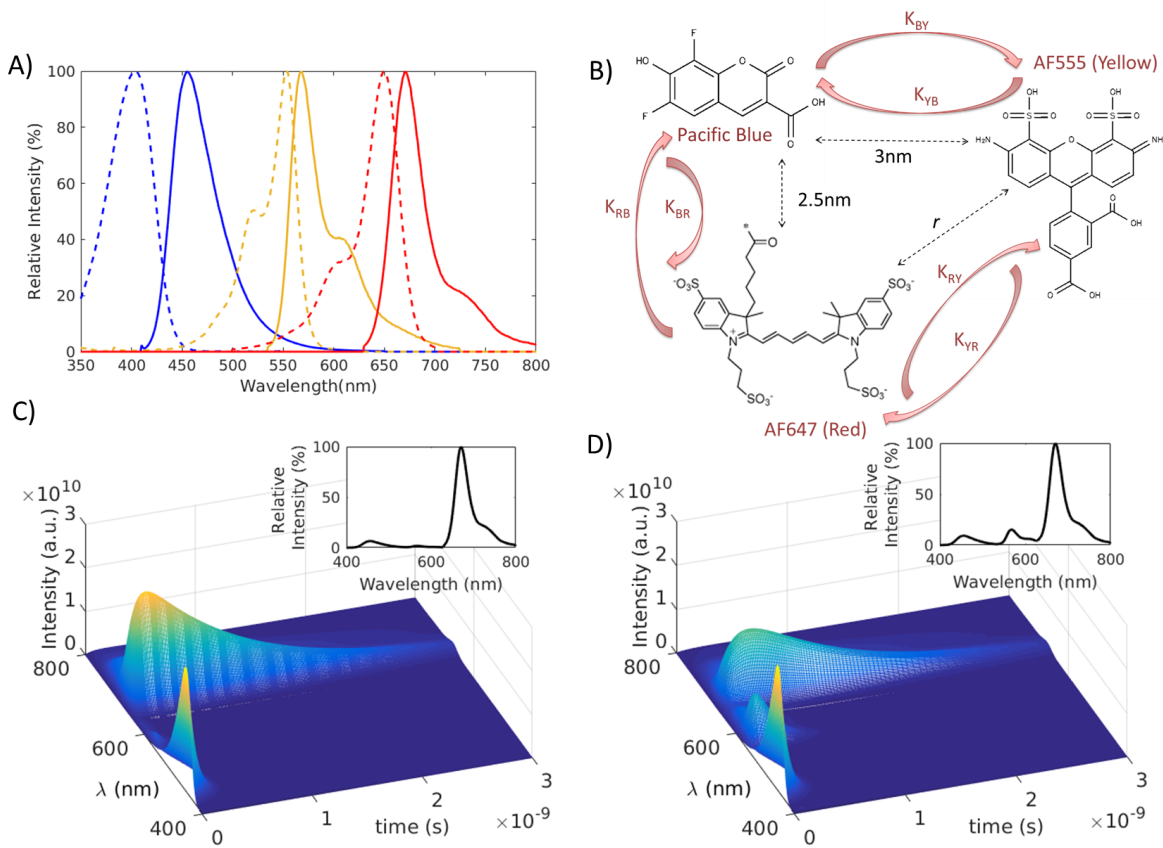


Figure 1: Absorption (dotted line) and emission (solid line) spectra of the three chromophores: Pacific Blue, Alexa Fluor 555 (AF555) and Alexa Fluor 647 (AF647), the spectra were taken from the Invitrogen website^[20]. B) Energy transfer pathways between the three dyes in a triangular geometry. Structures of Pacific Blue and AF555 were taken from ChEBI database^[22]. C-D) Time and frequency resolved fluorescence spectra of the chromophore network for two different spatial arrangements of the three dyes: $r=3\text{nm}$ (C) and $r=5\text{nm}$ (D).

3. The random walk of excitons and the outputting of the arrival time distribution

The exciton hopping dynamics described by the Förster theory can be formalized as a continuous time Markov chain (CTMC). Markov chains are stochastic processes $\{X(t) : t \geq 0\}$ where the random variable $X(t)$ is the state occupied by the chain at time t . The times between successive transitions are independent exponential random variables with means that depend only on the state from which the transition is being made. To build the state space of the CTMC that corresponds to the exciton dynamics we associate three discrete states of the chain to each chromophore in the network: the i -th dye is described by the state I , representing its excited state, the state FI , corresponding to emission by fluorescence and the state GI identified with non-radiative decay of the excitation. Referring to the triad of dyes of figure 1B this description generates 9 states that we label as B, Y, R (excited states of

the blue, yellow and red dye, respectively), FB, FY and FR (emission of the photon with blue, yellow and red wavelength, respectively) and the states GB, GY and GR (non-radiative de-excitation to the ground state of each chromophore). Since the identity of the non-radiative decay states is not relevant for the dynamics nor for the calculation of the fluorescence signal we lump them together in a unique state of the chain that is labelled as G. The resulting state space of the chain is made of 7 states and the corresponding graph is shown in figure 2A. The absorption of one photon initialize the chain in one of the excited states (B,Y or R depending on the excitation wavelength). The created exciton is a walker that explores the graph according to a set of probabilistic rules. The edges of the graph are labelled by the transition rates that determines the probability, $P_{ab}(t)$, of moving from one node of the graph to the others

$$\text{Prob}\{X(s+t) = a | X(s) = b\} = \Pi_{ab}(t) \quad (4)$$

for all states a, b and for all times $s > 0$ and $t > 0$. The transition probabilities are independent on s (because we are dealing with a stationary process) and they are explicitly given in matrix form as

$$\Pi(t) = \exp(\mathbf{Q}t) = \mathbf{I} + \mathbf{Q}t + \frac{1}{2}\mathbf{Q}^2t^2 + \dots \quad (5)$$

where \mathbf{Q} is the analog of the rate matrix \mathbf{K} for the populations in eq. (1), but in the basis of the 7 states of the Markov chain, that is

$$\mathbf{Q} = \left[\begin{array}{ccc|c} & \mathbf{K} & & \mathbf{0}_{3 \times 4} \\ \hline \Gamma_B & 0 & 0 & \\ 0 & \Gamma_Y & 0 & \mathbf{0}_{4 \times 4} \\ 0 & 0 & \Gamma_R & \\ \hline \mathbf{K}_{nr,B} & \mathbf{K}_{nr,Y} & \mathbf{K}_{nr,R} & \end{array} \right] \quad (6)$$

where the states are ordered as (B, Y, R, FB, FY, FR, G). Notice that the transition matrix eq. (5) involves all the powers of the infinitesimal generator of the process \mathbf{Q} . In practice, if we choose to discretize time^[23] the first order approximation works well for a small time interval h

$$\Pi_{ij}(h) = \delta_{ij} \left[1 - \sum_l Q_{li}h \right] + Q_{ij}h + O(h^2) \quad (7)$$

Excited states B, Y and R are transient states of the chain having both incoming and outgoing edges. The remaining states FB, FY, FR and G are absorbing states for which $\Pi_{ii} = 1$, meaning that when the walker hits one of these states it cannot leave it. A main result concerning absorbing Markov chains states that, no matter where the process starts, the probability after n transitions that the chain is in an absorbing state tends to 1 as n tends to infinity. The physical meaning of this theorem in our system is clear: before or later the created exciton recombines irreversibly either by emission of a photon or by non radiative dissipation. The time dependent probability of the states is given by the solution of the rate equation

$$\frac{d\mathbf{P}(t)}{dt} = \mathbf{Q}\mathbf{P}(t) \quad (8)$$

which gives

$$\mathbf{P}(t) = \mathbf{\Pi}(t)\mathbf{P}(0) \quad (9)$$

Figure 2B) shows the evolution of the probability of each state of the Markov chain describing the chromophore triad by assuming that at $t=0$ only Pacific Blue (B) is excited, using the topology of Figure 1C. Shortly after excitation, the probability of remaining in the excited state B drops exponentially while the probability of the excited states of the yellow and the red dyes increase because of the possible energy transfer from the blue dye. As the time increases, probability of being in any excited state tends to zero while the probabilities of having emitted a photon of a specific color (dashed colored lines) or having decayed non radiatively (dashed black line) approach their steady state values. From the solution of eq.(8), the probability of photon emission from the dye i up to time t reads

$$P_{Fi}(t) = \Gamma_i \int_0^t P_i(t') dt' \quad (10)$$

For $t \rightarrow \infty$ the steady state probability P_{Fi}^{st} of being absorbed in the state Fi determines the intensity of fluorescence measured in steady state condition at the emission wavelength of the i -th dye

$$I_\infty(\lambda_i^{em}) = \lim_{t \rightarrow \infty} P_{Fi}(t) = P_{Fi}^{st} \quad (11)$$

When no inter-chromophoric energy transfer processes are active, the steady state population of the fluorescence state corresponds to the quantum yield of the dye. Notice that the sum of the steady

state probabilities of the absorbing states is one. The time resolved signal is proportional to the (un-normalized) probability density of the walker to hit the F_i state at a given time instant. This is obtained as the time derivative of eq. (10), that is

$$I(\lambda_i^{em}, t) = \frac{dP_{F_i}(t)}{dt} = \Gamma_i P_i(t) \quad (12)$$

Therefore we recover the direct proportionality of the time resolved fluorescence emission on the transient population of the excited states, eq.(3).

Strictly speaking, equation (8) that defines the random walk of the exciton gives the probability over the possible states upon the absorption of a single photon. We might ask what is the relation between such a description and the probability of detecting n photons emitted by dye i up to time t , $p(n, t)$, which is the quantity experimentally accessible in a photon counting experiment. It turns out that if we excite the system N times and we can consider the random walk of each exciton as independent (condition that can be achieved by setting properly the rate of the excitation pulses), then the number of detected photons follows a binomial distribution

$$p(n, t) = \binom{N}{n} P_{F_i}(t)^n (1 - P_{F_i}(t))^{N-n} \quad (13)$$

The average number of detected photon is thus simply $\langle n(t) \rangle = NP_{F_i}(t)$ while the deviation from the average scaled as \sqrt{N} , ensuring that working with the average is a good approximation which is getting better as the number of collected photons increases. To illustrate this point, figure 2C shows the average time resolved emission from the red dye calculated according eq. (12) (dotted line) and the photon counts obtained by the simulation of 10^4 (black staircase) and 10^7 (red staircase) absorption events. In conclusion, we showed that the dynamics of the excitons through the chromophoric network realizes a physical random walk on the corresponding state space. Time resolved fluorescence spectra encodes information not only on the probability of ending up in a specific absorbing state but also on the time that it will likely take to reach such a state. In the next section, we will use this information to show that a properly designed network can be used to solve a real life-like problem.

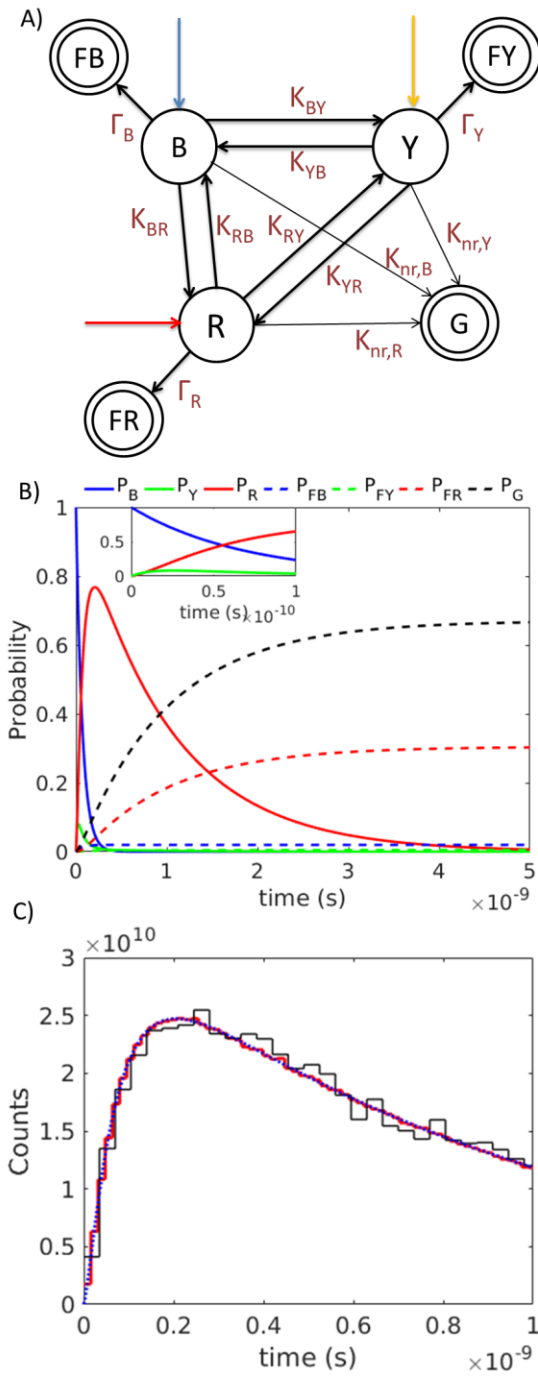


Figure 2: A) graphical representation of the CTMC implemented by three chromophores. B) Time evolution of the probabilities of the states of the Markov chain, in the inset a magnification of the short time behavior is shown. C) Time resolved fluorescence signal at the emission wavelength of the red chromophore (668nm): blue dotted line is the asymptotic signal, black staircase line is the photon counts obtained with 10^4 photons and red staircase line is the counts obtained with 10^7 photons.

4. Analysis of multiple travelling pathways

We are now in the position of exploiting the random walk of exciton in the multi-chromophore network for logic processing. To illustrate the potentialities of the CTMC inherently implemented in our system we will formulate the problem in the following terms: a professor is invited to give a talk at the University of Munich but for the scheduled day only flights for Milan and for Paris are available. Therefore, she will have to land in one of these two cities and then reach Munich by other means. The driving distance between Paris and Munich is 826 km while Milan is closer with a driving distance of 557 km. However, there is a fast train line between Paris and Munich and not between Milan and Munich. Where should the professor land?

The problem is implemented in our chromophore triad spatially arranged as shown in the upper scheme of Figure 3A) where Pacific Blue (B) represents Milan, AF555(Y) Paris and AF647 (R) is Munich. The relative distance between the chromophores r_{ij} reflects the driving distance between the cities. The presence of a fast train line between Paris and Munich is physically encoded by the longer Förster distance of the Y-R pair ($R_{0,RY} = 51\text{Å}$) compared to the B-R pair ($R_{0,RB} = 37.5\text{Å}$). Remember that the transfer rate between two dyes j and i is determined by a combination of the two parameters r_{ij} and $R_{0,ij}$ according to eq.(2). In the corresponding CTMC (see figure 2A) the starting states of the chain are either B (Milan) or Y (Paris) that can be populated selectively by exciting the system at their specific excitation wavelength. The state FR represents the professor safely arrived in Munich so that the relevant output is the fluorescence at the emission wavelength of the red dye. In particular, the intensity of the steady state fluorescence spectra at $\lambda=668\text{nm}$ is directly proportional to the total probability of arriving in Munich, eq.(11), while the time-resolved fluorescence emission gives the probability density of arrival at a certain time t , eq. (12). Figure 3B shows the time resolved fluorescence signal from the red dye for the two different excitation conditions as input (solid line “a” for the excitation of the yellow dye, and “b” for the excitation of the blue dye). The fluorescence response encodes the analysis of the arrival probability in Munich of our travelling professor. While the total probability of arriving (proportional to the integral of the time resolved signal) is practically independent on the starting city (0.305 starting from Milan against 0.309 starting from Paris), the time resolved signal shows that the travelling time is likely to be shorter when starting from Paris. Let us now suppose that the fast line train connecting Paris to Munich has some trouble because of an accident. The probability to get stuck in Paris then increases and we have to update the transition

probability of the CTMC accordingly. One way to do so is to increase the distance between the yellow and the red chromophore as depicted in the bottom scheme of figure 3A, resulting in a smaller transfer rate according to eq.(2). The corresponding fluorescence output is shown in figure 3B (dashed lines c and d). In this second case starting from Milan assures a higher value of the maximum probability density and a higher total probability of ever arriving in Munich. However, the most likely arrival time is still longer than by starting from Paris. Based on these results the traveler Professor will make her choice. The time dependent fluorescence signal of the multi-chromophore system offers a rather detailed analysis of the efficiency of different travelling pathways. Figures 3C and D show the total arrival probability, the maximum value of the probability density and the corresponding arrival time starting from the two different locations (Paris or Milan) as a function of the distance between the Yellow and the Red chromophores r . The modulation of this distance is only one of the parameters that can be changed to simulate several situations affecting the relative transfer rates.^[12c] Other distances, the chemical nature of the chromophores, the presence of quenchers and changes in the chemical environment represents other controllable parameters that can be used to program the Markov chain that is implemented by the system.

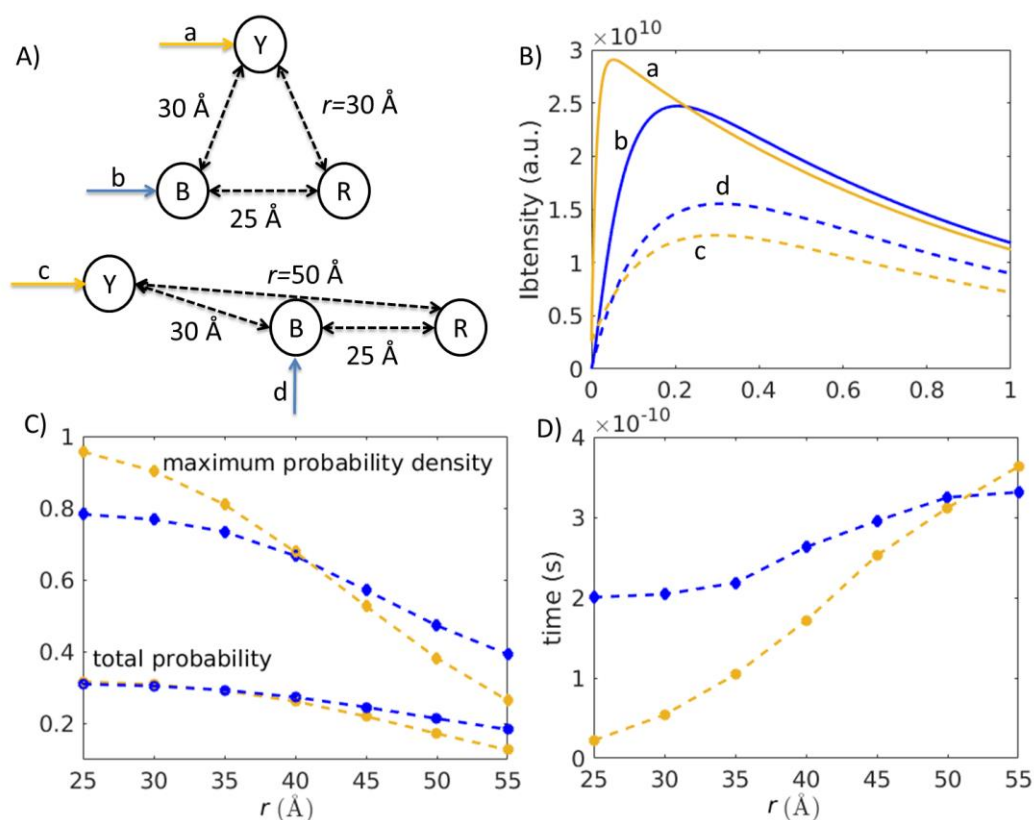


Figure 3: A) scheme of two geometrical arrangements of the chromophore triad and B) corresponding time resolved emission at the emission wavelength of the red chromophore (668nm) for two excitation conditions: selective excitation of the blue chromophore (blue lines) and selective excitation of the yellow chromophore (yellow lines). C) Total probability and maximum probability density of arriving in the state of the chain FR by starting from the state B (blue line) and Y (yellow line) as a function of the distance r between the yellow and the red dyes. D) Arrival time corresponding to the maximum of the probability density.

5. Concluding Remarks

We showed that exciton transfer dynamics in multi-chromophore molecular aggregates implements at the hardware level a Markov chain performing a random walk through a network. Non-trivial information about the possible pathways of the random walk, namely the probability of hitting different absorbing states and the time likely required to reach these states depending on the starting condition is encoded in the experimentally accessible time resolved fluorescence spectra. By selecting the dye molecules and controlling their spatial arrangement, the molecular device can be programmed to simulate Markov chains addressing specific problems. We discussed the solution of a prototype problem requiring the analysis of different pathways that a traveler can take to reach a target city. Limitations on the implementable network topologies are imposed by the tridimensional structures of the molecular system that are realizable. Even if this is still a small fraction of the infinite variety of possible topologies, the capability of designing and synthesizing multi-chromophore structures make them promising building blocks for the efficient implementation of probabilistic algorithms. Experimental realization of molecular devices built by assembling DNA bricks in programmable nanobreadboards on which chromophores can be rapidly and easily repositioned has been recently demonstrated.^[12a] An important point to consider in the practical implementation of the proposed logic scheme is the overlap between the spectral features of the different chromophores. Ideally, the dyes which we want to selectively excite and the target dye whose populations needs to be monitored in time should have absorption and emission wavelengths, respectively, that are distinct from the others. When this is not strictly realizable, a complete photo-physical characterisation of the system is required to estimate the specific chromophore contribution to the collected signal. To evaluate the effective FRET rates, a suitable averaging procedure should be implemented, depending on the relative timescales of the dye rotational and translational dynamics relative to the FRET timescale. Indeed, the orientation factor κ influencing the rate of the excitation transfer between two interacting dyes adopts a range of values depending on the dye configurations sampled. In our model,

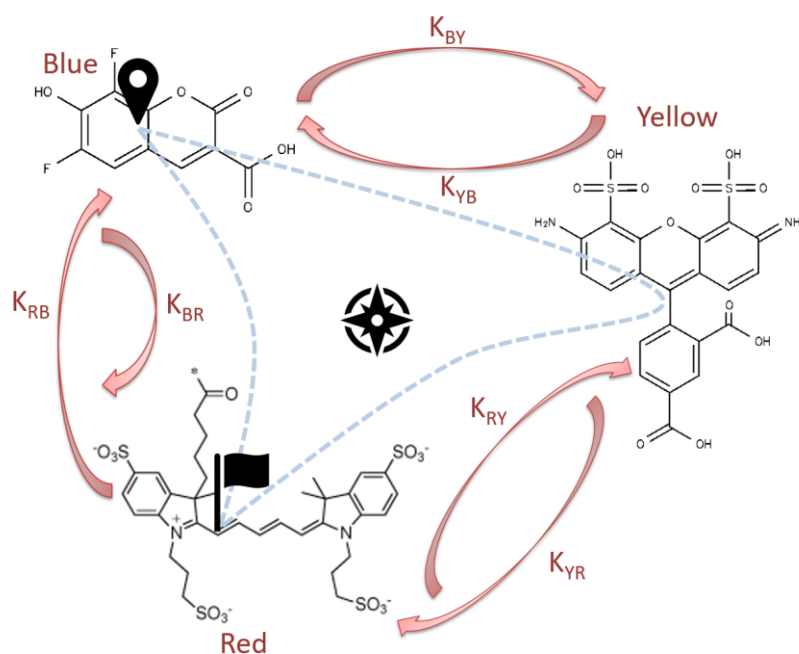
we consider dyes which are covalently conjugated to nucleotides via C3 or C6 flexible linkers, for which isotropic averaging is appropriate in most cases and $\kappa = 2/3$. However, other fluorescent probes have been designed for allowing the control of both their position and mutual orientation, such as the tC dye family,^[24] intercalating dyes from the YO (oxazole yellow) and TO (thiazole orange) families and intercalated and covalently-conjugated porphyrins^[25]. The control over relative orientations allows enhancing or suppressing the rate of specific energy transfer pathways by changing the value of the orientation factor κ and it is another means to tune the rate parameters of the random walk dynamics.

Our implementation of probabilistic algorithms points out that molecular devices can perform logic functionalities that go far beyond the execution of molecular gates. Further developments of this idea are expected to emerge by considering the optical response at the single molecule level.^[26] By measuring the emission of single FRET pairs, a distribution of energy transfer efficiency is obtained rather than its average value.^[27] This might empower the logic capabilities of the molecular system, for example by allowing the introduction of a degree of uncertainty on the parameters of the logic problem. However, this possibility will come at the cost of a less straightforward interpretation of the output. Coherent energy transfer may additionally emerge when chromophores interact at close range, requiring quantum mechanical modeling and allowing the implementation of quantum stochastic walk.^[28] New features stemming from quantum mechanical coherences and single molecule detection will be the subject of future research.

Acknowledgements

BF acknowledges the support of the Italian Ministero dell'Istruzione, Università e Ricerca through the grant Rita Levi Montalcini – 2013 and FR the support of Fonds National de la Recherche Scientifique, FRS-FNRS, Belgium. BF thanks Prof. Camilla Ferrante for useful insights on time resolved fluorescence detection techniques.

TOC graphics



A probabilistic algorithm implemented in a molecular system shows that molecular devices can have logic functionalities going beyond the execution of binary gates. The hopping dynamics of excitons in a multi-chromophore system (see figure) realizes a random walk that samples the possible pathways of a traveler and outputs useful information through the time-resolved fluorescence signal.

References

- [1] a) R. Motwani, P. Raghavan, *Randomized Algorithms*, Cambridge University Press, **1995**; b) T. L. Booth, *Sequential Machines and Automata Theory*, John Wiley and Sons, Inc., **1967**.
- [2] F. Li, K. Shim, K. Zheng, G. Liu, *Web Technologies and Applications: 18th Asia-Pacific Web Conference, APWeb 2016, Suzhou, China, September 23-25, 2016. Proceedings*, Springer International Publishing, **2016**.
- [3] a) M. Rosvall, C. T. Bergstrom, *Proc. Natl. Acad. Sci. U.S.A.* **2008**, *105*, 1118-1123; b) C. C. Aggarwal, *Social Network Data Analytics*, Springer US, **2011**.
- [4] a) K. C. Chipman, A. K. Singh, *BMC Bioinformatics* **2009**, *10*, 17; b) W. Peng, J. Wang, Z. Zhang, F. Wu, *Curr. Bioinform.* **2016**, *11*, 211-220.
- [5] A. Sinclair, *Algorithms for Random Generation and Counting: A Markov Chain Approach*, Birkhäuser Boston, **1993**.
- [6] B. Fresch, J. Bocquel, S. Rogge, R. D. Levine, F. Remacle, *Nano Lett.* **2017**.
- [7] a) C. Javier, A. M. José, M. Salvador, *Nanotechnology* **2009**, *20*, 465202; b) C. Javier, A. M. José, M. Salvador, *Nanotechnology* **2011**, *22*, 435201; c) B. Fresch, H.-G. Boyen, F. Remacle, *Nanoscale* **2012**, *4*, 4138-4147; d) B. Fresch, E. Hanozin, F. Dufour, F. Remacle, *EPJ D* **2012**, *66*; e) B. Fresch, F. Remacle, *J. Phys. Chem. C* **2014**, *118*, 9790-9800.
- [8] a) S. Buckhout-White, J. C. Claussen, J. S. Melinger, Z. Dunningham, M. G. Ancona, E. R. Goldman, I. L. Medintz, *RSC Adv.* **2014**, *4*, 48860-48871; b) B. Fresch, D. Hiluf, E. Collini, R. D. Levine, F. Remacle, *Proc. Natl. Acad. Sci. U.S.A.* **2013**, *110*, 17183-17188; c) T.-M. Yan, B. Fresch, R. D. Levine, F. Remacle, *J. Chem. Phys.* **2015**, *143*; d) M. F. Budyka, V. M. Li, *ChemPhysChem* **2017**, *18*, 260-264; e) L. Olejko, P. J. Cywinski, I. Bald, *Nanoscale* **2016**, *8*, 10339-10347; f) B. Fresch, M. Cipolloni, T.-M. Yan, E. Collini, R. D. Levine, F. Remacle, *J. Phys. Chem. Lett.* **2015**, *6*, 1714-1718.
- [9] M. D. Mottaghi, C. Dwyer, *Adv. Mater.* **2017**, *25*, 3593-3598.
- [10] Y. N. Teo, E. T. Kool, *Chem. Rev.* **2012**, *112*, 4221-4245.
- [11] a) P. K. Dutta, S. Levenberg, A. Loskutov, D. Jun, R. Saer, J. T. Beatty, S. Lin, Y. Liu, N. W. Woodbury, H. Yan, *J. Am. Chem. Soc.* **2014**, *136*, 16618-16625; b) P. K. Dutta, R. Varghese, J. Nangreave, S. Lin, H. Yan, Y. Liu, *J. Am. Chem. Soc.* **2011**, *133*, 11985-11993; c) J. S. Melinger, R. Sha, C. Mao, N. C. Seeman, M. G. Ancona, *J. Phys. Chem. B* **2016**, *120*, 12287-12292; d) J. G. Woller, J. K. Hannestad, B. Albinsson, *J. Am. Chem. Soc.* **2013**, *135*, 2759-2768.
- [12] a) B. L. Cannon, D. L. Kellis, P. H. Davis, J. Lee, W. Kuang, W. L. Hughes, E. Graugnard, B. Yurke, W. B. Knowlton, *ACS Photonics* **2015**, *2*, 398-404; b) J. S. Melinger, A. Khachatryan, M. G. Ancona, S. Buckhout-White, E. R. Goldman, C. M. Spillmann, I. L. Medintz, P. D. Cunningham, *ACS Photonics* **2016**, *3*, 659-669; c) K. Pan, E. Boulais, L. Yang, M. Bathe, *Nucleic Acids Res.* **2014**, *42*, 2159-2170.
- [13] a) C.-H. Lu, B. Willner, I. Willner, *ACS Nano* **2013**, *7*, 8320-8332; b) J. Elbaz, O. Lioubashevski, F. Wang, F. Remacle, R. D. Levine, I. Willner, *Nat. Nanotech.* **2010**, *5*, 417-422; c) C. H. Lu, A. Ceconello, X. J. Qi, N. Wu, S. S. Jester, M. Famulok, M. Matthies, T. L. Schmidt, I. Willner, *Nano Lett.* **2015**, *15*, 7133-7137; d) J. Elbaz, A. Ceconello, Z. Fan, A. O. Govorov, I. Willner, *Nat. Commun.* **2013**, *4*, 2000; e) C.-H. Lu, A. Ceconello, J. Elbaz, A. Credi, I. Willner, *Nano Lett.* **2013**, *13*, 2303-2308.
- [14] a) P. Rothmund, *Nature* **2006**, *440*, 297-302; b) A. Pinheiro, D. Han, W. Shih, H. Yan, *Nat. Nanotechnol.* **2011**, *6*, 763-772.
- [15] B. Fresch, F. Remacle, *Phys. Chem. Chem. Phys.* **2014**, *16*, 14070-14082.
- [16] A. K. Luong, C. C. Gradinaru, D. W. Chandler, C. C. Hayden, *J. Phys. Chem. B* **2005**, *109*, 15691-15698.
- [17] a) T. Förster, *Ann. Phys.* **1948**, *437*, 55-75; b) T. Forster, *Disc. Faraday Soc.* **1959**, *27*, 7-17.

- [18] a) Y. R. Khan, T. E. Dykstra, G. D. Scholes, *Chem. Phys. Lett.* **2008**, *461*, 305-309; b) R. Ziessel, M. A. H. Alamiry, K. J. Elliott, A. Harriman, *Angew. Chem. Int. Ed.* **2009**, *48*, 2772-2776.
- [19] G. D. Scholes, *Ann. Rev. Phys. Chem.* **2003**, *54*, 57-87.
- [20] <http://www.thermofisher.com/it/en/home/life-science/cell-analysis/labeling-chemistry/fluorescence-spectraviewer.html>.
- [21] J. R. Lakowicz, *Principles of Fluorescence Spectroscopy*, Kluwer Academic/Plenum, **1999**.
- [22] J. Hastings, P. de Matos, A. Dekker, M. Ennis, B. Harsha, N. Kale, V. Muthukrishnan, G. Owen, S. Turner, M. Williams, C. Steinbeck, *Nucleic Acids Res.* **2013**, *41*, D456-463.
- [23] B. Doytchinov, R. Irby, *Pi Mu Epsilon Journal* **2010**, *13*, 69-82.
- [24] S. Preus, K. Kilså, F.-A. Miannay, B. Albinsson, L. M. Wilhelmsson, *Nucleic Acids Res.* **2013**, *41*, e18-e18.
- [25] L.-A. Fendt, I. Bouamaied, S. Thöni, N. Amiot, E. Stulz, *J. Am. Chem. Soc.* **2007**, *129*, 15319-15329.
- [26] a) F. Kulzer, M. Orrit, *Annu. Rev. Phys. Chem.* **2004**, *55*, 585-611; b) E. Barkai, Y. J. Jung, R. Silbey, *Annu. Rev. Phys. Chem.* **2004**, *55*, 457-507.
- [27] A. A. Deniz, M. Dahan, J. R. Grunwell, T. J. Ha, A. E. Faulhaber, D. S. Chemla, S. Weiss, P. G. Schultz, *Proc. Natl. Acad. Sci. U.S.A.* **1999**, *96*, 3670-3675.
- [28] a) J. D. Whitfield, C. A. Rodríguez-Rosario, A. Aspuru-Guzik, *Phys. Rev. A* **2010**, *81*, 022323; b) M. Mohseni, P. Rebentrost, S. Lloyd, A. Aspuru-Guzik, *J. Chem. Phys.* **2008**, *129*, 174106; c) F. Caruso, A. Crespi, A. G. Ciriolo, F. Sciarrino, R. Osellame, *Nat. Commun.* **2016**, *7*, 11682.